Supporting Information

Synthesis of new *N,N′*-Pd(Pt) complexes based on sulfanyl pyrazoles, and investigation of their *in vitro* anticancer activity

Vnira R. Akhmetova,*[a] Nail S. Akhmadiev,[a] Marat F. Abdullin,[b] Lilya U. Dzhemileva[a] and Vladimir A. D'yakonov[a]

[a]Institute of Petrochemistry and Catalysis, Russian Academy of Sciences, 141 Prospekt Oktyabrya, 450075 Ufa, Russian Federation. *E-mail: vnirara@mail.ru; Tel./fax: +7 3472 842750
[b]Ufa Institute of Chemistry, Russian Academy of Sciences, 71 Prospekt Oktyabrya, 450054 Ufa, Russian Federation.

Materials and methods

All synthesized compounds were characterized by ^{1}H and ^{13}C, ^{15}N NMR spectral data that were recorded on spectrometers Bruker Avance 400 NMR (400.13 MHz and 100.62 MHz) and Bruker Ascend III HD 500 (500.17 MHz and 125.78 MHz), internal standard TMS, solvent DMSO-D_6. IR spectra were recorded on a Bruker Vertex-70V FTIR and Specord M80 spectrometers. Matrix-assisted laser desorption/ionization (MALDI) mass spectrum was recorded on a Bruker's device MALDI TOF Autoflex III (compounds **7** and **8** in DMSO) with sinapinic acid as a matrix. Electrospray ionization (ESI) mass spectra were obtained on a HPLC mass spectrometer LCMS-2010EV (Shimadzu) in the positive and negative ions mode at the ionizing electrode potential of 4.5 kV and −3.5 kV, respectively. Elemental analysis was performed on a Carlo Erba 1106 elemental analyzer. Melting points were determined on a Kofler hot-stage microscope and utilized uncorrected. Individuality and purity of synthesized compounds were controlled by means of TLC on Silufol UV-254 plates; I_2 was used as developer. Synthesis of 4-[(sulfanyl)methyl]-3,5-dimethyl-1*H*-pyrazoles **4a-d** was carried out according to the procedure described previously.[1] The spectral characteristics of the obtained pyrazole ligands **4a-d** are consistent with published data.[1]

3,5-Dimethyl-4-[(phenylsulfanyl)methyl]-1*H*-pyrazole (4a). White powder. ^{1}H NMR spectrum (400 MHz, $CDCl_3$), δ, ppm: 2.17 (6H, s, CH_3); 3.94 (2H, s, CH_2); 7.24–7.37 (5H, m, H Ph); 10.93 (1H, br. s, NH).

4-[(Benzylsulfanyl)methyl]-3,5-dimethyl-1*H*-pyrazole (4b). White powder. ^{1}H NMR spectrum (400 MHz, $CDCl_3$), δ, ppm: 2.19 (6H, s, CH_3); 3.49 (2H, s, $PhCH_2S$); 3.69 (2H, s, SCH_2); 7.25–7.35 (5H, m, H Ph); 10.32 (1H, br. s, NH).

4-[(Cyclohexylsulfanyl)methyl]-3,5-dimethyl-1*H*-pyrazole (4c). White powder, ^{1}H NMR spectrum (400 MHz, $CDCl_3$), δ, ppm: 1.26–1.40 (4H, m, CH_2); 1.60–1.64 (2H, m, CH_2); 1.76–1.79 (2H, m, CH_2); 1.97–2.00 (2H, m, CH_2); 2.28 (6H, s, CH_3); 2.52–2.60 (1H, m, CHS); 3.57 (2H, s, SCH_2); 10.63 (1H, br. s, NH).

4-{[(3,5-Dimethyl-1*H*-pyrazol-4-yl)methyl]sulfanyl}-phenol (4d). White powder, ^{1}H NMR spectrum (400 MHz, DMSO-D_6), δ, ppm (J, Hz): 1.95 (6H, s, CH_3); 3.76 (2H, s, SCH_2); 6.69 (2H, d, *J* = 8.0, H Ar), 7.12 (2H, d, *J* = 8.0, H Ar); 9.60 (1H, s, OH); 11.99 (1H, br. s, NH).

A known pharmaceutical drug, cisplatin, manufactured by Bayer Pharma AG (Germany), with *cis*-diaminedichloridoplatinum(II) as the active substance, was used as the reference drug.

Synthesis of the N,N′-complexes of palladium(II) ***5a,b*** *and* ***6a,b***. Palladium(II) chloride (0.05 g, 0.28 mmol) or palladium(II) bromide (0.07 g, 0.28 mmol) was dissolved in acetonitrile

(15 mL) with stirring at 60 °C in the glass vessel. Then the appropriates 3,5-dimethyl-4-((sulfanyl)methyl)-1*H*-pyrazoles **4b** or **4c** (0.56 mmol) was added and stirred at rt (~20 °C) for 3 h. The resulting bright yellow precipitate was filtered through filter paper (blue ribbon) and washed by acetonitrile (30 mL), water (30 mL) and dried in air without heat to obtain *N,N´*-complexes of palladium(II).

Dichlorobis-[(4-(benzylsulfanyl)methyl)-3,5-dimethyl-1*H*-pyrazole]palladium (5a). Yellow powder. Yield (0.15 g, 83%). M.p. (dec.) 176 – 178 °C. Found: C, 48.79; H, 5.23; Cl, 11.13; N, 8.62; S, 9.83. Anal. Calc. for $C_{26}H_{32}Cl_2N_4PdS_2$: C, 48.64; H, 5.02; Cl, 11.04; N, 8.73; Pd, 16.58; S, 9.99. IR (Nujol, cm^{-1}): ν = 3470 (s), 1584 (s), 1299 (s), 1198 (m), 724 (m), 477 (s), 362 (s), 341 (s). ^{1}H-NMR (ppm) δ 13.24 (s, NH), 7.25 – 7.33 (m, Ar), 3.69 (s, SC$\underline{H}_2$Ph), 3.48 (s, PzC$\underline{H}_2$S), 2.52 (s, CH_3), 2.13 (s, CH_3). ^{13}C-NMR (ppm) δ 9.5, 13.3, 23.9, 36.0, 113.3, 127.3, 128.9, 129.2, 138.6, 141.6, 148.8. ^{15}N-NMR (ppm) δ 195.8 and 200.7 (NH). MS (ESI), m/z (I, %): 646 (65) $[M\text{-}Cl+CH_3CN]^+$.

Dibromobis-[(4-(benzylsulfanyl)methyl)-3,5-dimethyl-1*H*-pyrazole]palladium complex (5b). Yellow powder. Yield (0.13 g, 65%). M.p. (dec.) 166 – 168 °C. Found: C, 42.87; H, 4.46; N, 7.48; S, 8.91; Br, 21.73. Anal. Calc. for $C_{26}H_{32}Br_2N_4PdS_2$: C, 42.73; H, 4.41; N, 7.67; Pd, 14.56; S, 8.77; Br, 21.86. IR (Nujol, cm^{-1}): ν = 3469 (s), 3079 (m), 1295 (s), 710 (m), 477 (m), 382 (s), 359 (s), 278 (m). ^{1}H-NMR (ppm) δ 13.21 (s, NH), 7.21 – 7.29 (m, Ar), 3.62 (s, SC$\underline{H}_2$Ph), 3.44 (s, PzC$\underline{H}_2$S), 2.48 (s, CH_3), 2.09 (s, CH_3). ^{13}C-NMR (ppm) δ 9.5, 13.9, 23.9, 35.8, 113.5, 127.3, 128.9; 129.2, 138.6, 141.9, 149.1. ^{15}N-NMR (ppm) δ 177.0 and 205.0 (NH). MS (ESI), m/z (I, %): 690 (52) $[M\text{-}Br+CH_3CN]^+$.

Dichlorobis-[(4-(cyclohexylsulfanyl)methyl)-3,5-dimethyl-1*H*-pyrazole]palladium complex (6a). Yellow powder. Yield, (0.14 g, 82%). M.p. (dec.) 192-194 °C. IR (cm^{-1}): ν = 3468 (s), 3161 (m), 2714 (m), 1587 (s), 1308 (s), 1204 (m), 846 (m), 773 (s). ^{1}H-NMR (ppm) δ 13.20 (s, NH), 3.56 (s, PzC$\underline{H}_2$S), 2.58 (s, CHS), 2.21 and 2.18 (s, CH_3), 1.90 – 1.93, 1.68 – 1.69, 1.54 – 1.56, 1.23 – 1.28 (m, CH_2). ^{13}C-NMR (ppm) δ 9.6, 13.4, 22.3, 25.8, 33.5, 43.3, 114.0, 141.3, 148.7. MS (ESI), m/z (I, %): 589 (41) $[M\text{-}Cl]^+$, 630 (59) $[M\text{-}Cl+CH_3CN]^+$.

Dibromobis-[(4-(cyclohexylsulfanyl)methyl)-3,5-dimethyl-1*H*-pyrazole]palladium complex (6b). Yellow powder. Yield (0.17 g, 85%). M.p. (dec.) > 250 °C. IR (Nujol, cm^{-1}): ν = 3244 (s), 1578 (s), 1196 (s), 820 (s), 658 (s), 580 (s), 508 (s), 321 (s). ^{1}H-NMR (ppm) δ 13.19 (s, NH), 3.56 (s, PzC$\underline{H}_2$S), 2.58 (s, CHS), 2.22 (s, CH_3), 1.89 – 1.93, 1.68 – 1.69, 1.54 – 1.56, 1.23 – 1.25 (m, CH_2). ^{13}C-NMR (ppm) δ 9.6, 13.9, 22.3, 25.8, 33.6, 43.2, 114.1, 141.6, 148.9. MS (ESI), m/z (I, %): 674 (56) $[M\text{-}Br+CH_3CN]^+$, 791 (48) $[M+Br]^-$.

Synthesis of N,N´-platinum complexes. Potassium tetrachloroplatinate (0.12 g, 0.28 mmol) was dissolved in water (5 mL) at room temperature (~20 °C) in the glass vessel and stirring vigorously on a magnetic stirrer, then a solution of the appropriate 3,5-dimethyl-4-((sulfanyl)methyl)-1*H*-pyrazoles **4b** or **4c** (0.56 mmol) in acetone (10 mL) was added. The mixture was stirred for 3 h, and then evaporated with gentle heating acetone. The resulting precipitate was washed with water, hexane and air-dried to give complex **7** and **8**.

Dichlorotri-[(4-(benzylsulfanyl)methyl)-3,5-dimethyl-1*H*-pyrazole]platinum complex (7). Light yellow powder. Yield (0.14 g, 71%). M.p. (dec.) 86 – 88 °C. IR (Nujol, cm^{-1}): ν = 3446 (s), 3162 (s), 1580 (s), 1206 (m), 1071 (s), 701 (m), 504 (s), 477 (s), 342 (s), 310 (m). ^{1}H-NMR (ppm) δ 13.81 (s, NH), 7.23 – 7.32 (m, Ar), 3.65 and 3.69 (s, SC$\underline{H}_2$Ph), 3.48 and 3.53 (s, PzC$\underline{H}_2$S), 2.31 and 2.34 (s, CH_3), 2.06 and 2.15 (s, CH_3). ^{13}C-NMR (ppm) δ 9.6, 10.7, 13.1, 23.9, 24.5, 35.5, 36.0, 113.5, 127.2, 127.3, 128.8, 128.9, 129.2, 138.6, 138.9, 141.3, 147.9. ^{15}N-NMR (ppm) δ 170.3 and 192.6 (NH), 179.6 and 206.1 (NH). MS (MALDI TOF) 926.6899 $[M\text{-}Cl]^+$; MS (ESI), m/z (I, %): 926 (87) $[M\text{-}Cl]^+$.

Dichlorotri-[(4-(cyclohexylsulfanyl)methyl)-3,5-dimethyl-1*H*-pyrazole]platinum complex (8). Light yellow powder. Yield (0.12 g, 60%). M.p. 102 – 104 °C. IR (Nujol, cm^{-1}): ν = 3445 (s), 3191 (m), 1585 (s), 1203 (m), 1037 (s), 722 (m). ^{1}H-NMR (ppm) δ 13.79 (s, NH), 3.53 (s, PzC$\underline{H}_2$S), 2.54 (s, CHS), 2.12 (s, CH_3), 1.90 – 1.94, 1.68 – 1.69, 1.54 – 1.55, 1.24 – 1.28 (m, CH_2). ^{13}C-NMR (ppm) δ 9.7; 13.1, 22.8, 26.0, 33.6, 42.9, 111.6, 141.8, 147.8. MS (MALDI TOF) 903.3284 $[M\text{-}Cl]^+$; MS (ESI), m/z (I, %): 902 (76) $[M\text{-}Cl]^+$, 819 (19) $[M\text{-}Cl\text{-}C_6H_{11}]^+$.

X-ray crystallography

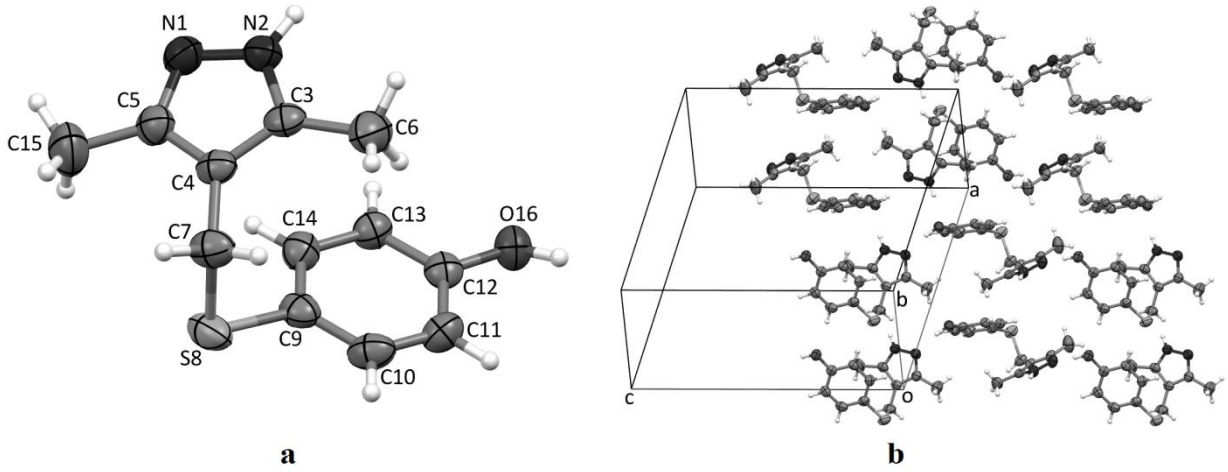

Fig. 2 The geometry of molecules of compound **4d** in a crystal (a). Atoms are represented by thermal ellipsoids (*p* = 50%). Packing of the **4d** molecules in their respective unit cell (b).

All diffraction measurements were performed at room temperature (298 K) using graphite monochromated Mo-Kα radiation (λ = 0.71073 Å) on a Agilent Xcalibur (Eos, Gemini) single-crystal diffractometer. Collection and processing of data performed with using the program CrysAlis^{Pro} Oxford Diffraction Ltd. The structures were structure was solved with the ShelXS[2] structure solution program using Direct Methods and refined with the ShelXL[3] refinement package using Least Squares minimization. The structure was refined by a full-matrix least-square technique using anisotropic thermal parameters for non-hydrogen atoms. The H16 atom in structure **4d** was located in a difference Fourier map and refined isotropically, and the other H atoms were positioned geometrically and treated using a riding model, fixing the bond lengths at 0.960, 0.970, 0.930 and 0.860 Å for CH_3, CH_2, CH and NH atoms, respectively. Atomic coordinates, bond lengths, bond angles, and thermal parameters have been deposited at the Cambridge Crystallographic Data Centre (www.ccdc.cam.ac.uk/data_request/cif). The crystallographic data for compound **4d** are collected in Table S1.

Table S1 Crystal data and structure refinement for compound **4d.**

CCDC	1954607
Empirical formula	$C_{12}H_{14}N_2OS$
Formula weight	234.31
Temperature/K	293(2)
Crystal system	monoclinic

Space group	C2/c
a/Å	19.1997(11)
b/Å	7.7319(4)
c/Å	16.5888(10)
α/°	90
β/°	95.914(5)
γ/°	90
Volume/$Å^3$	2449.5(2)
Z	8
$\rho_{calc}g/cm^3$	1.271
μ/mm^{-1}	0.245
F(000)	992.0
Radiation	MoKα (λ = 0.71073)
2Θ range for data collection/°	4.266 to 58.278
Index ranges	$-26 \leq h \leq 24$, $-6 \leq k \leq 10$, $-19 \leq l \leq 22$
Reflections collected	5838
Independent reflections	2802 [R_{int} = 0.0215]
Data/restraints/parameters	2802/0/151
Goodness-of-fit on F^2	1.041
Final R indexes [I>=2σ (I)]	R_1 = 0.0461, wR_2 = 0.1180
Final R indexes [all data]	R_1 = 0.0644, wR_2 = 0.1323
Largest diff. peak/hole / e $Å^{-3}$	0.22/-0.26

Cell culturing

Jurkat, K562, and U937 cells were received from the Russian Collection of Cell Cultures (Institute of Cytology, Russian Academy of Sciences, St.-Petersburg). The cells were cultured in the RPMI 1640 complete medium (Biolot) containing 10% of fetal calf serum; 2 mM of L-glutamine; 50 U/mL of penicillin; and 50 μg/mL of streptomycin. HEK293 cell line was cultured as monolayers and maintained in Dulbecco's modified Eagle's medium (DMEM, Gibco BRL) supplemented with 10% fetal bovine serum and 1% penicillin-streptomycin solution. The cells were cultured in vials in a CO_2 incubator at a temperature of 37°C, a 5% CO_2 atmosphere, and a saturation humidity. The cell viability was studied for 5th to 10th passage cells. For experiments, the suspension cell cultures that have reached the logarithmic growth phase were subcultured into 24-well plates (100 thousand cells per well). After addition of test compounds, the cells were incubated for 24 h and the results were analyzed by flow cytometry.

Evaluation of cell viability

The cell viability was evaluated by flow cytometry using 7-AAD (7-aminoactinomycin D), a fluorescent DNA dye (Sony Biotechnology Inc.). This dye cannot penetrate living cells with undamaged, intact membranes.

The intensity of 7-AAD fluorescence in the BL-4 channel (PerCP) was evaluated on a NovoCyteTM 2000 flow cytometer (ACEA). The instrument was adjusted against control samples including living unstained cells (estimation of autofluorescence), living cells stained with 7AAD with no dye uptake and low fluorescence level (gating of living cells), and cells

incubated under the same conditions with compounds inducing cell death (gating of dead cells). In each sample, at least 1×10^4 cells were measured. If dead cells are present, the cell population is cytometrically subdivided into two groups: living cells show a low fluorescence level, whereas dead cells have high fluorescence intensity.

Study of apoptosis

The quantitative analysis of apoptosis-inducing activity was performed using Alexa Fluor® 488 Annexin V/Dead Cell Apoptosis Kit, with fluorescence being recorded on a NovoCyteTM 2000 flow cytometer (ACEA). Phosphatidylserine externalization on the plasmatic membrane surface is a reliable sign of cell apoptosis or necrosis. Normally functioning living cells have a minor amount of phosphatidylserine on the outer cell membrane and, hence, the interaction with Alexa Fluor® 488 annexin V is insignificant. In addition, undamaged cell membrane is impermeable for propidium iodide. In early apoptosis, phosphatidylserine molecules appear on the cell surface; however, the membrane is still impermeable for dyes that bind to DNA (such as propidium iodide). The membrane integrity is damaged at later stages of cell death. Thus, when apoptosis is detected, four types of cells are distinguished: living cells (annexin V- / PI -), early apoptotic cells (annexin V + / PI-), late apoptotic cells (annexin V + / PI +), and necrotic cells (annexin V- / PI +).

Interaction between DNA plasmid pHOT and tested compounds

The reaction mixture (20 μL) containing 0.25 μg of the DNA plasmid pHOT (TopoGen, USA), and the tested compound was incubated in the buffer (35mM Tris-HCl, pH 8.0; 72 mM KCl, 5 mM MgCl, 5 mM dithiothreitol, 5 mM spermidine, and 0,01% bovine serum albumin) for 30 min at 37°C using a Biosan thermostat (Latvia). The reaction was terminated by adding sodium dodecyl sulfate up to a concentration of 1%. A 0.1% solution of bromophenol blue (1:10) was added and the samples were electrophoresed in the presence of ethidium bromide. The reaction products were separated in a 1% agarose gel (3 V/cm) for 4-6 h. After the electrophoresis without ethidium bromide, the gels were treated with a solution of ethidium bromide (0.5 μg/mL). The gels were visualized in the UV light in a Infinity VX2 1120/Blue X-Press gel documentation system (Vilber Lourmat, France).

References

1 N. S. Akhmadiev, V. R. Akhmetova, T. F. Boiko and A. G. Ibragimov, Nickel-catalyzed multicomponent heterocyclization of 2,4-pentanedione to sulfanylmethyl-1H-pyrazoles, *Chem. Heterocycl. Compound.*, 2018, **54**, 344–350 (Eng. Transl.). https://doi.10.1007/s10593-018-2271-5.

2 G. M. Sheldrick, A short history of SHELX, *Acta Cryst.*, 2008, **A64**, 112–122. https://doi.org/10.1107/S0108767307043930.

3 G. M. Sheldrick, Crystal structure refinement with SHELXL, *Acta Cryst.*, 2015, **C71**, 3–8. http://dx.doi.org/10.1107/S205322961402421.

Fragments of the NMR, IR, mass-spectra

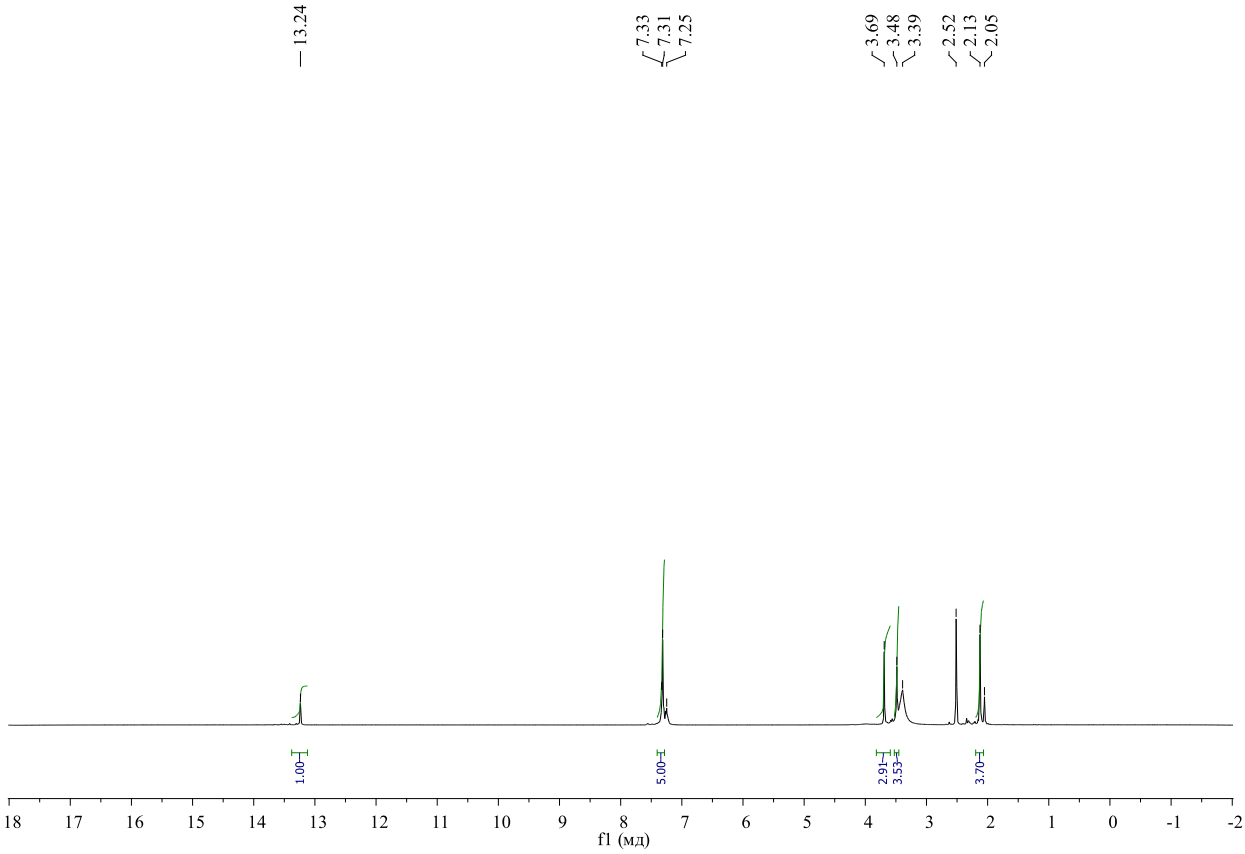

Fig. S1. ^{1}H NMR spectrum of complex **5a** ($BnPzPdCl_2$) in DMSO-D_6 (400 MHz)

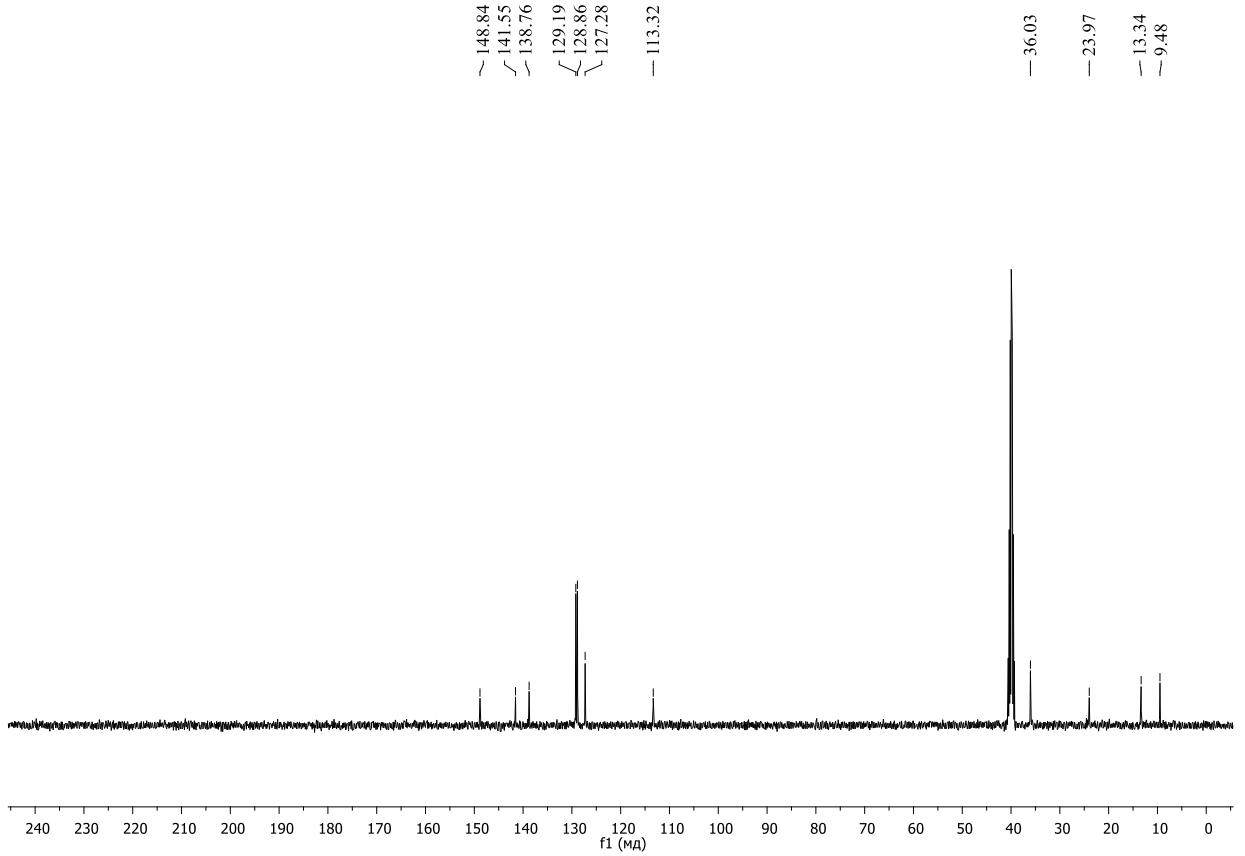

Fig. S2. ^{13}C NMR spectrum of complex **5a** ($BnPzPdCl_2$) in DMSO-D_6 (100 MHz)

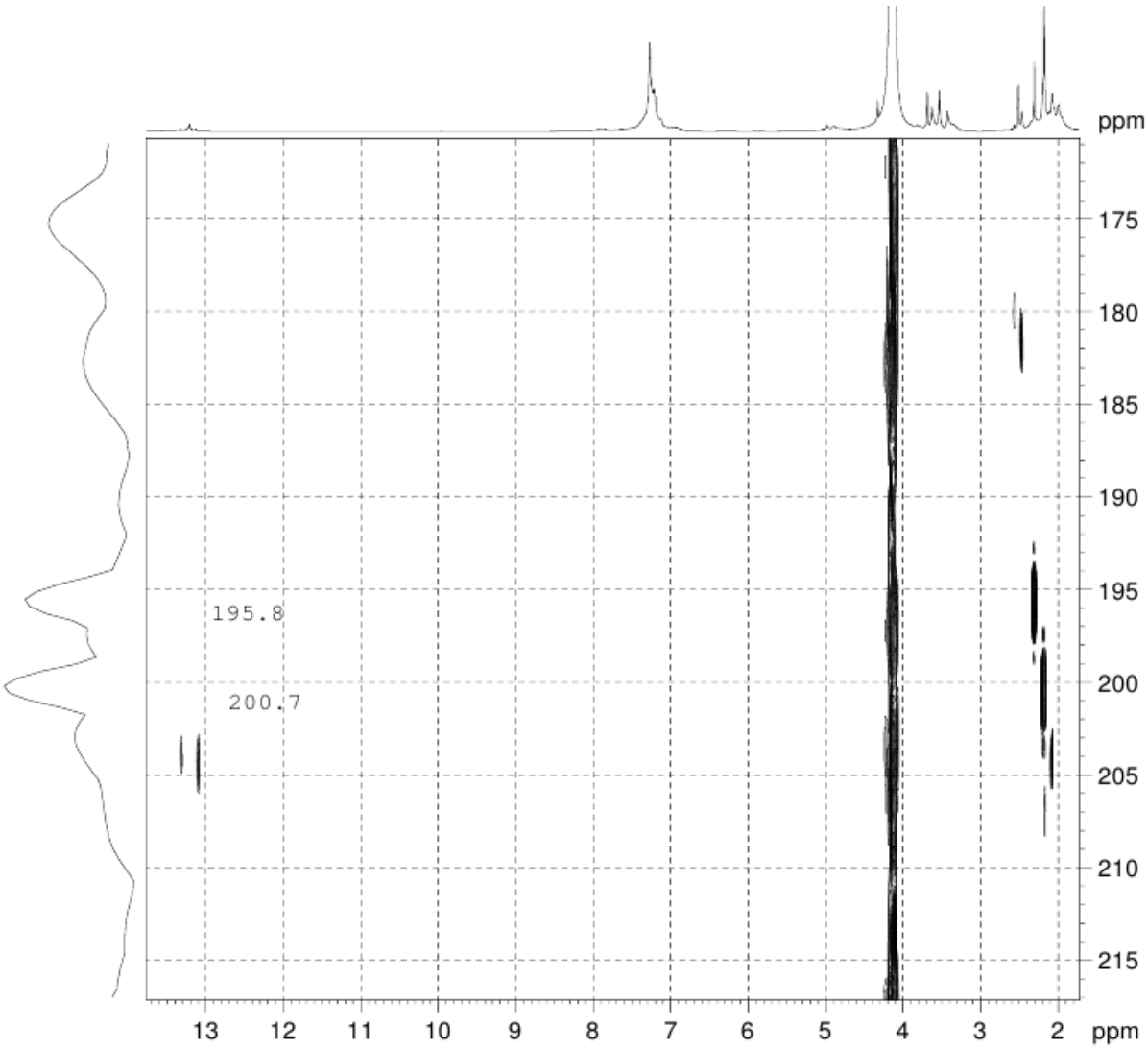

Fig. S3. ^{1}H-^{15}N-HMBC spectrum of complex **5a** ($BnPzPdCl_2$) in DMSO-D_6 (500 MHz)

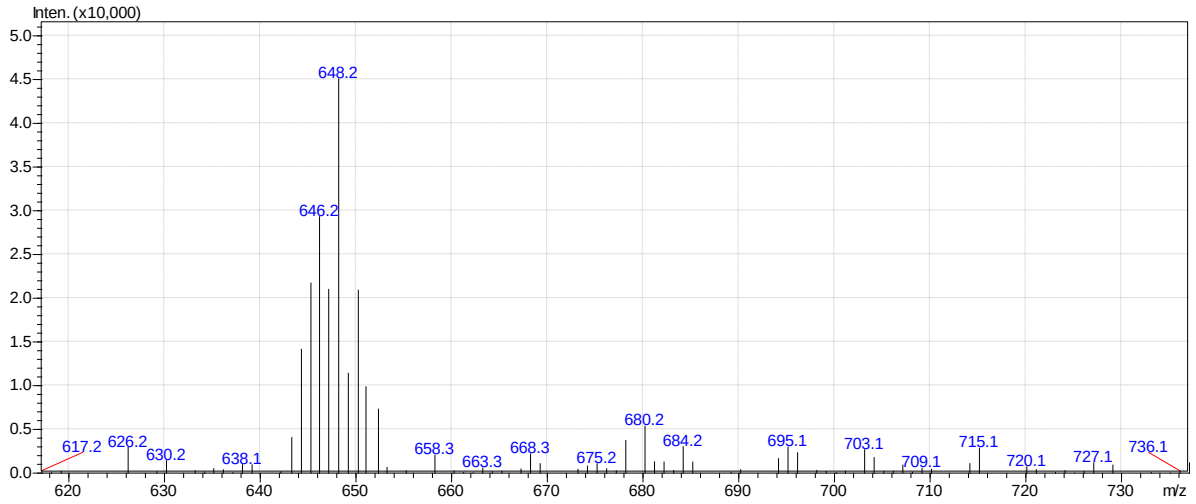

Fig. S4. Positive ion ESI mass spectrum of compound **5a**.

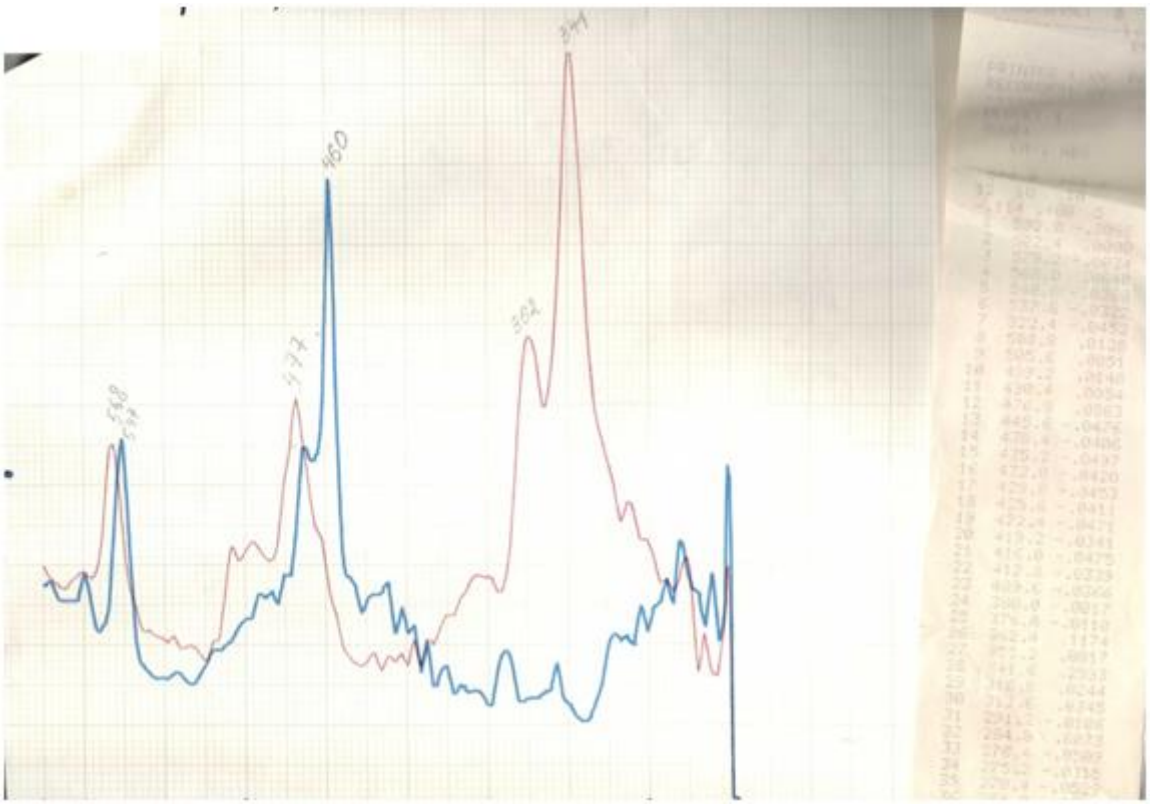

Fig. S5. IR **s**pectrum of complex **5a** in nujol: (blue line – **4b**, red line – complex **5a**).

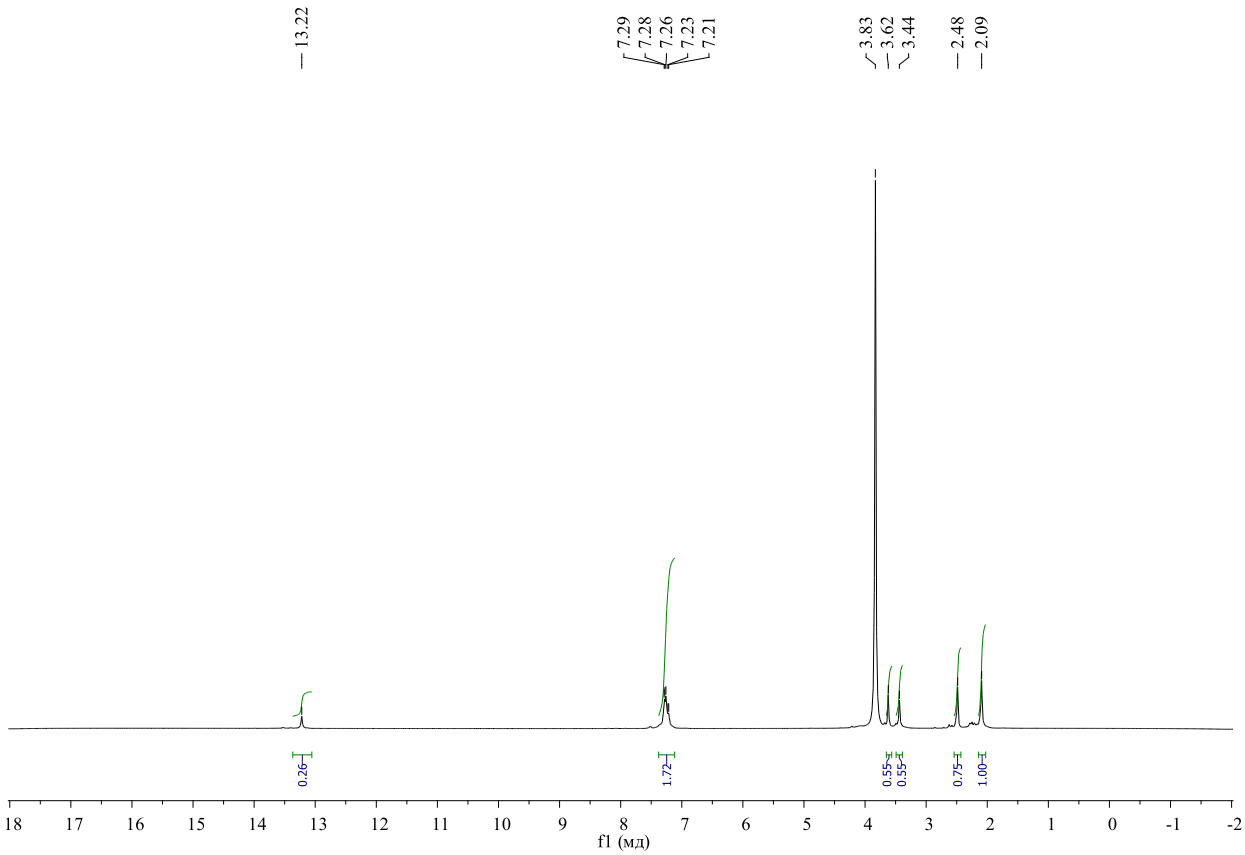

Fig. S6. ^{1}H NMR spectrum of complex **5b** ($BnPzPdBr_2$) in DMSO-D_6 (400 MHz)

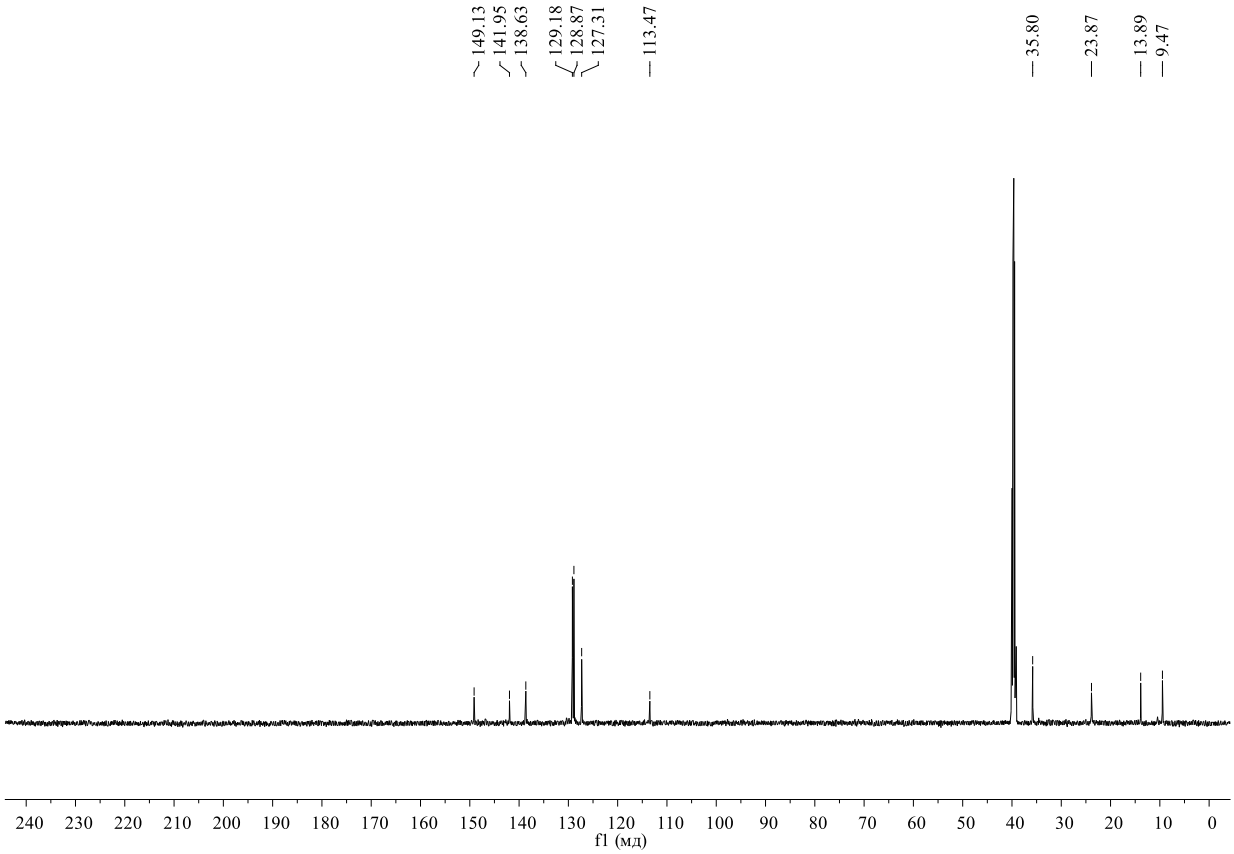

Fig. S7. ^{13}C NMR spectrum of complex **5b** ($BnPzPdBr_2$) in DMSO-D_6 (100 MHz)

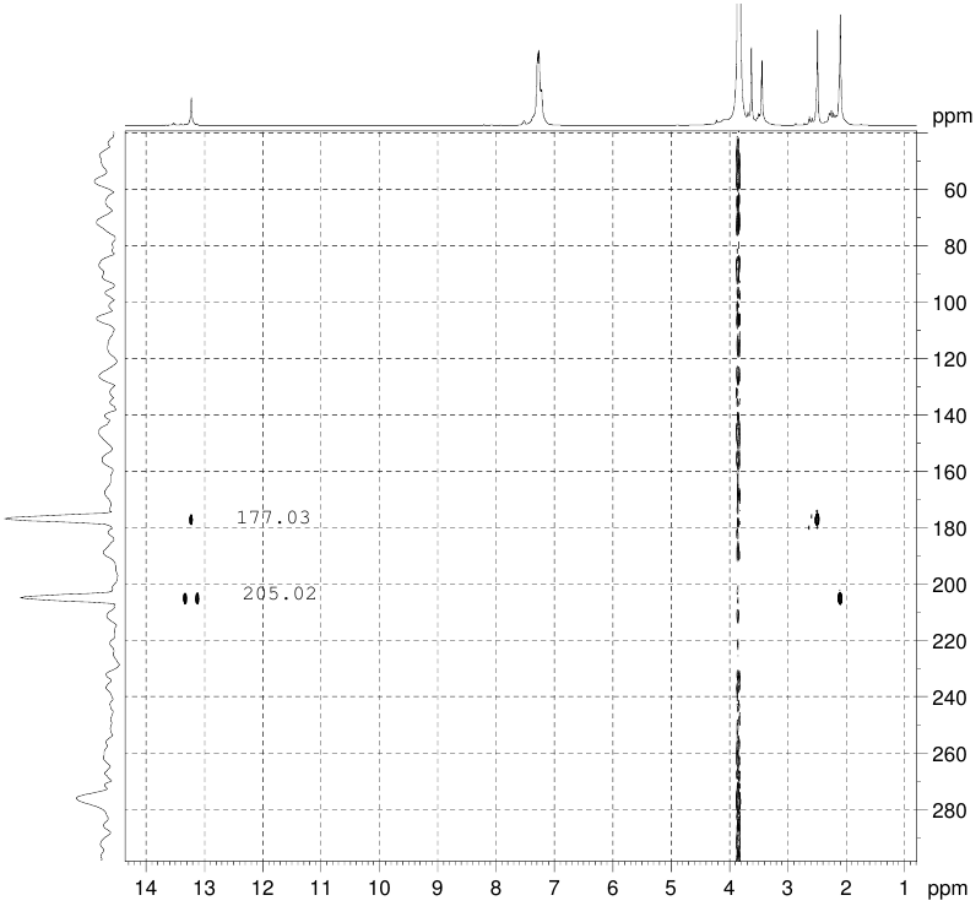

Fig. S8. ^{1}H-^{15}N-HMBC spectrum of complex **5b** ($BnPzPdBr_2$) in DMSO-D_6 (500 MHz)

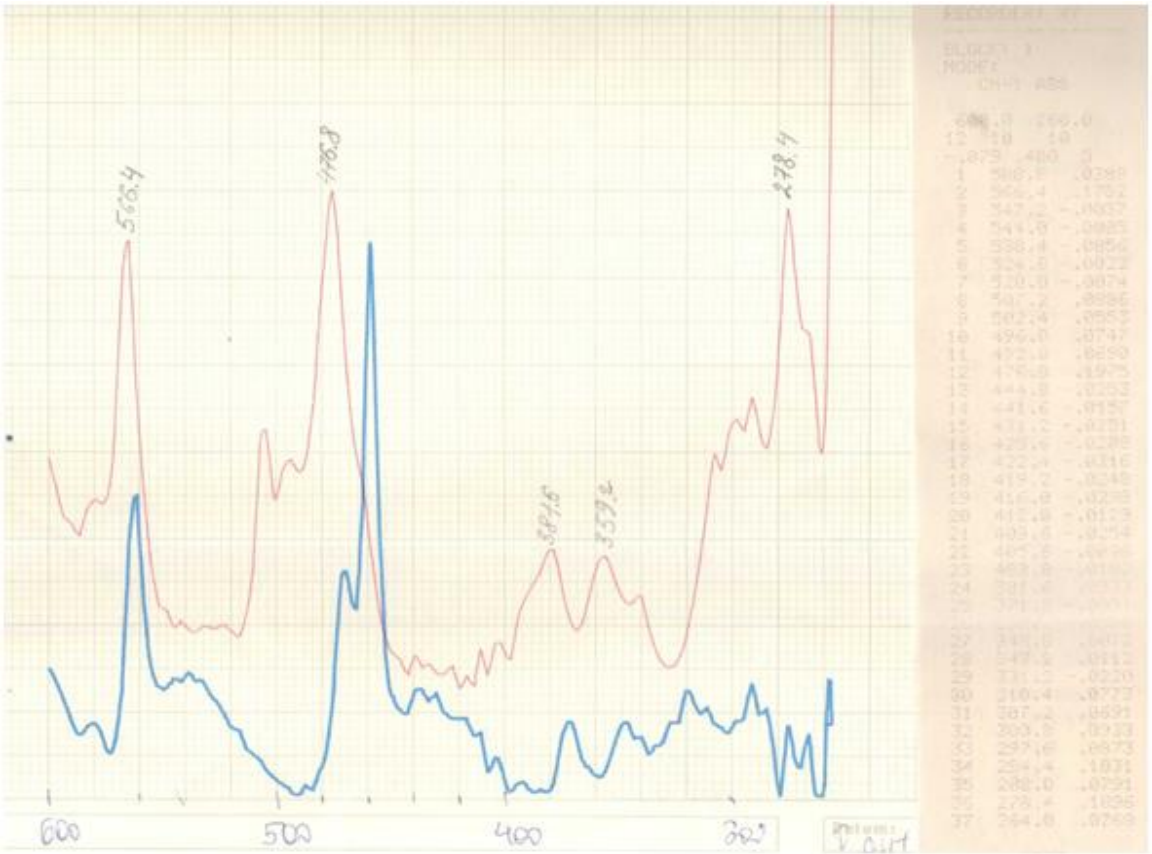

Fig. S9. IR spectrum of complex **5b** in nujol: (blue line – **4b**, orange line – complex **5b**).

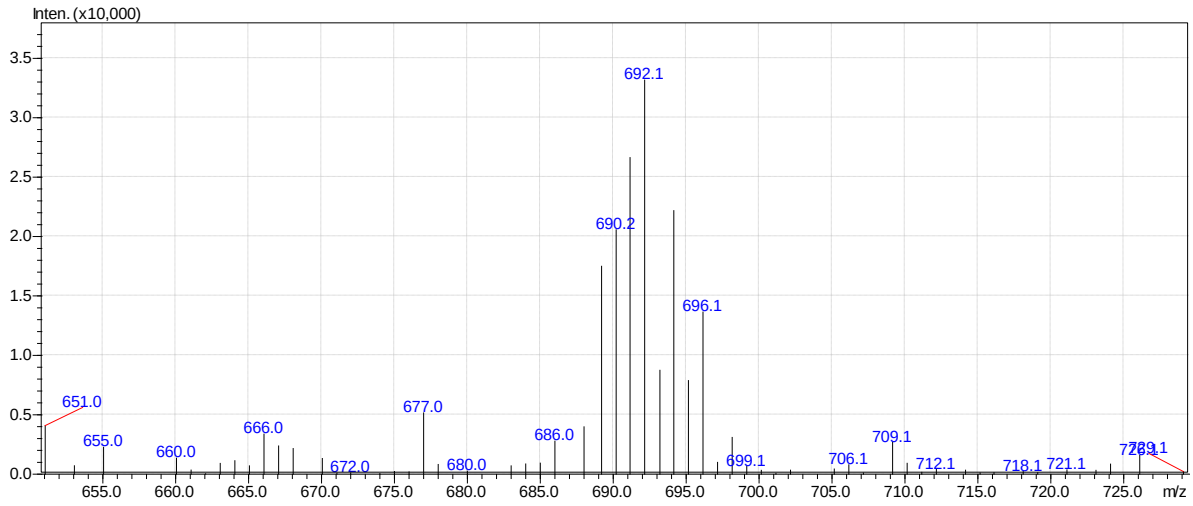

Fig. S10. Positive ion ESI mass spectrum of compound **5b**.

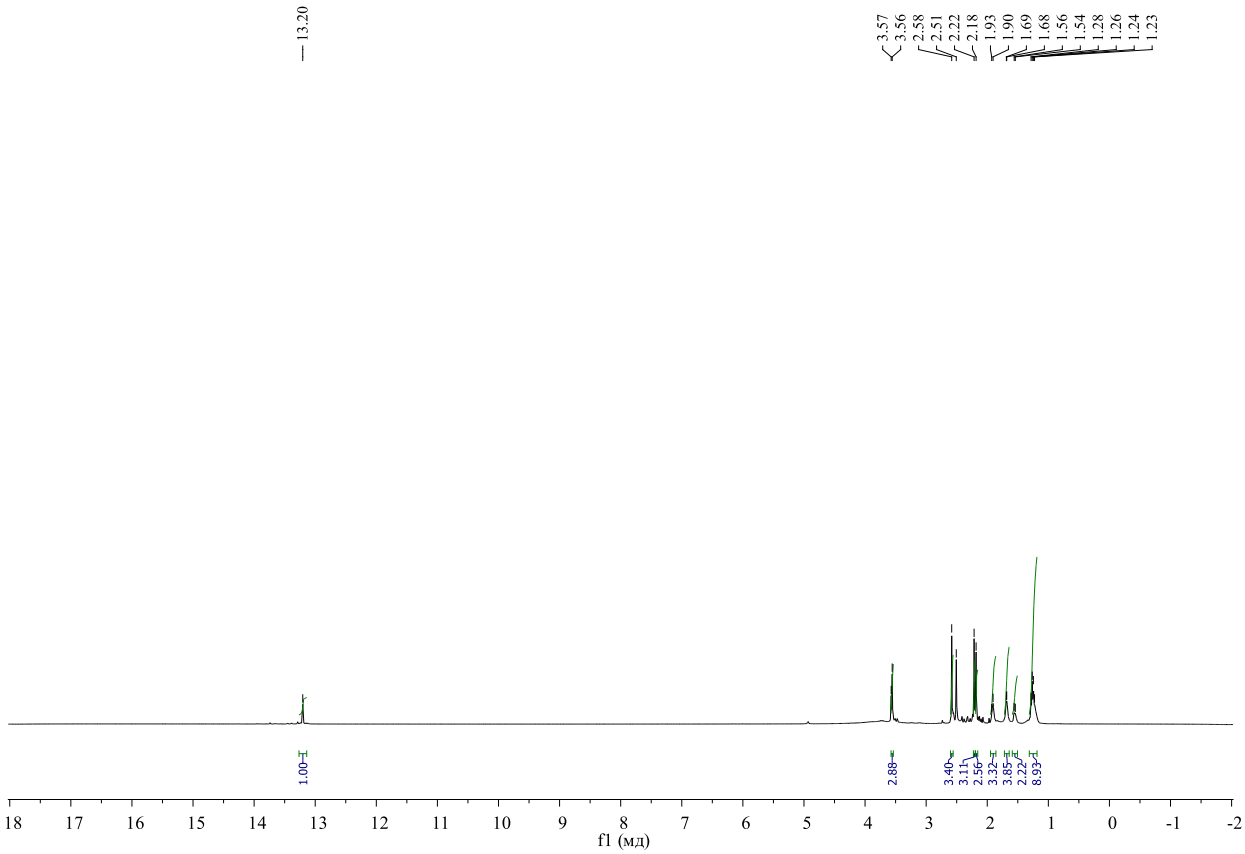

Fig. S11. ^{1}H NMR spectrum of complex **6a** ($CyPzPdCl_2$) in DMSO-D_6 (500 MHz)

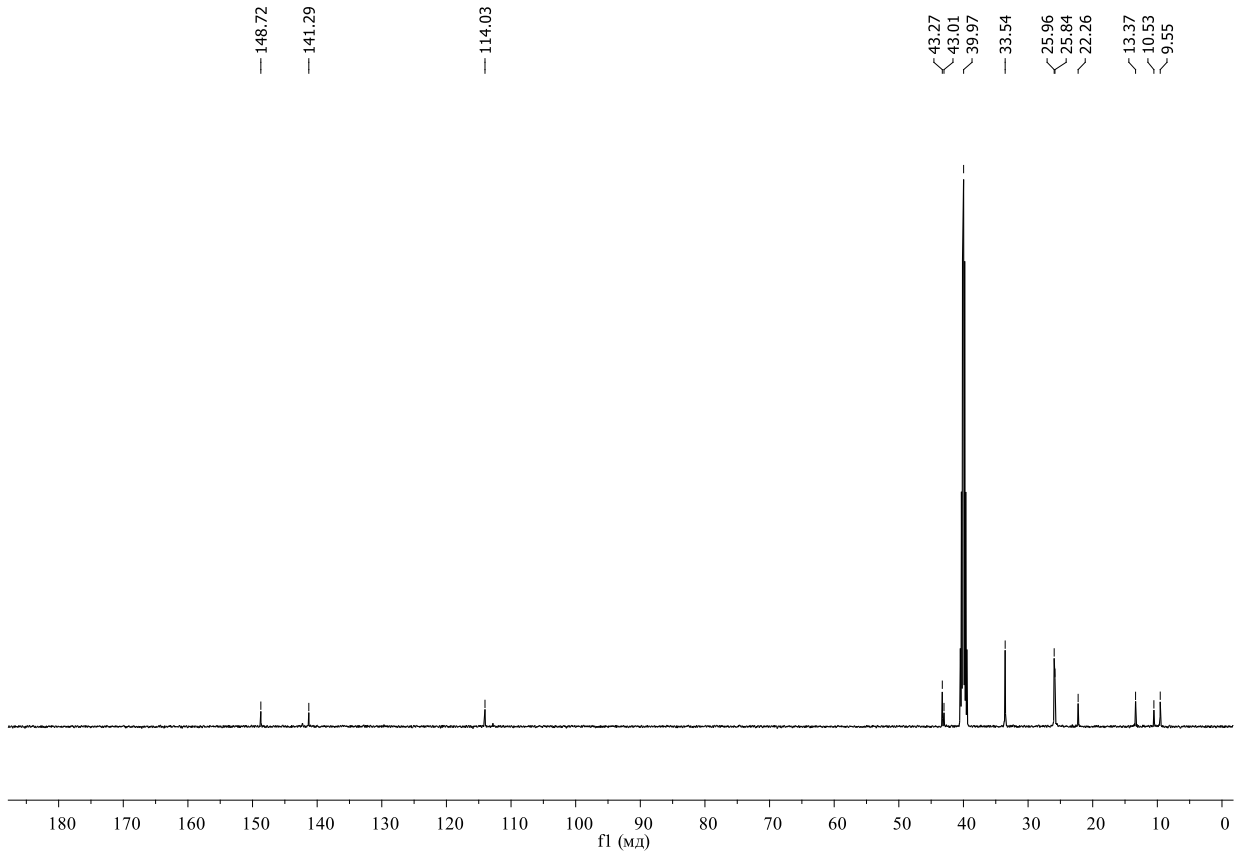

Fig. S12. ^{13}C NMR spectrum of complex **6a** ($CyPzPdCl_2$) in DMSO-D_6 (125 MHz)

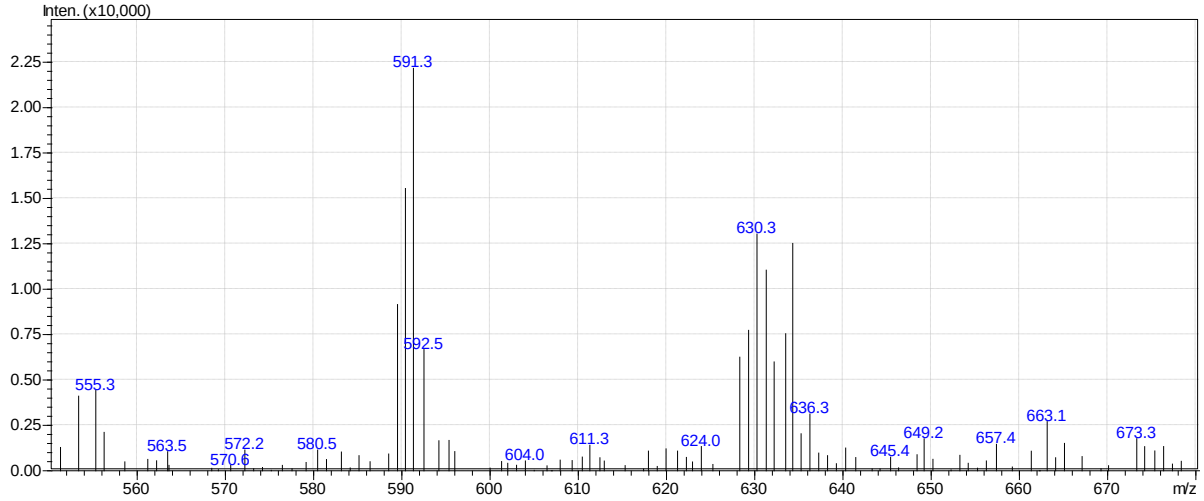

Fig. S13. Positive ion ESI mass spectrum of compound **6a**.

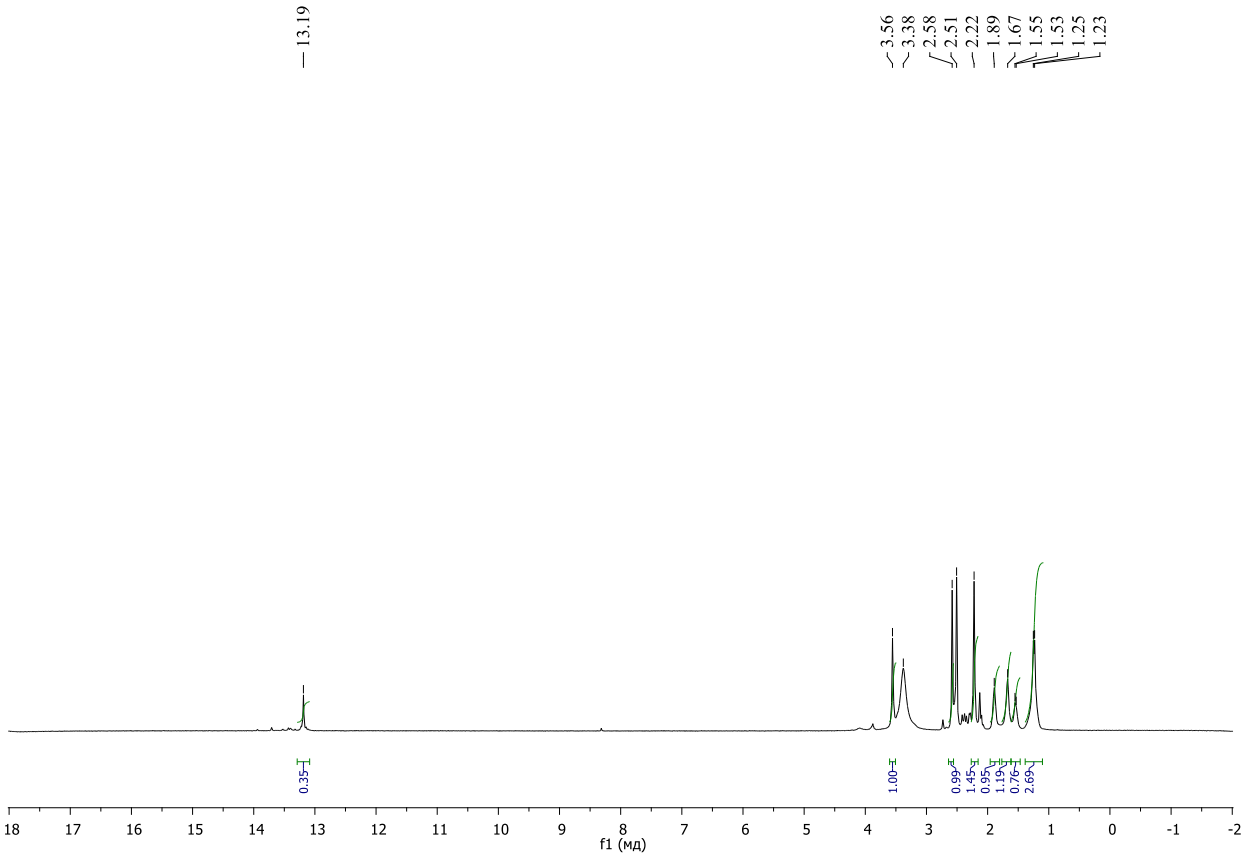

Fig. S14. ^{1}H NMR spectrum of complex **6b** ($CyPzPdBr_2$) in DMSO-D_6 (400 MHz)

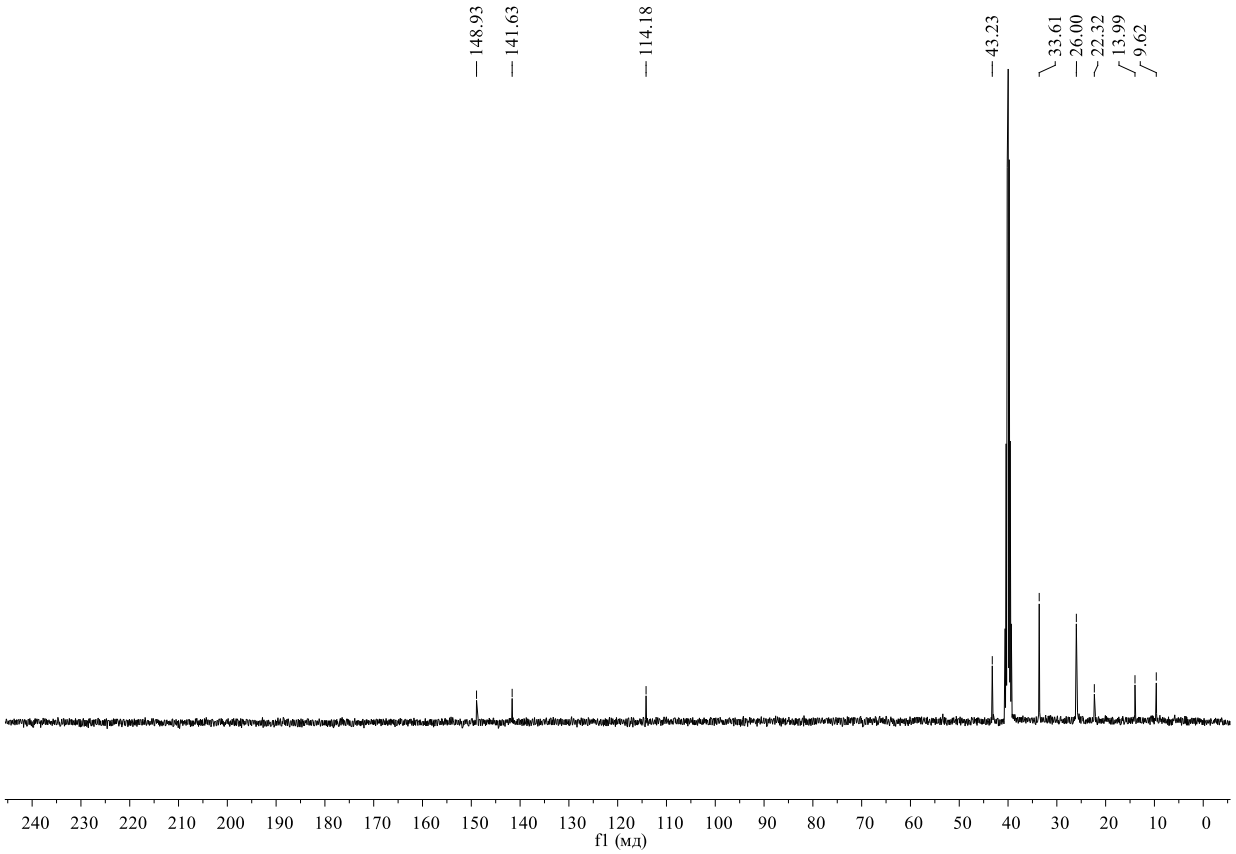

Fig. S15. ^{13}C NMR spectrum of complex **6b** ($CyPzPdBr_2$) in DMSO-D_6 (100 MHz)

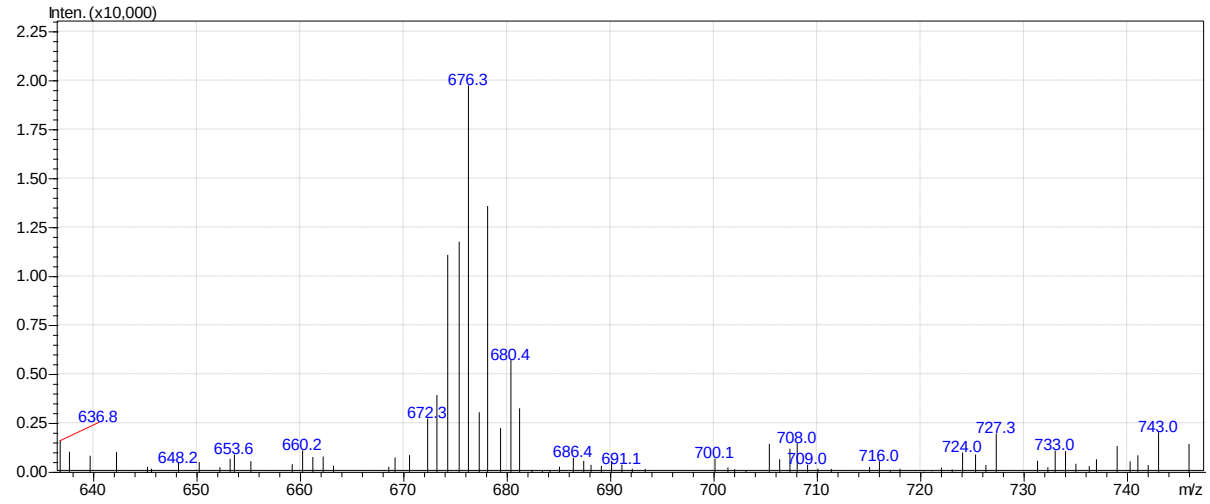

Fig. S16. Positive ion ESI mass spectrum of compound **6b.**

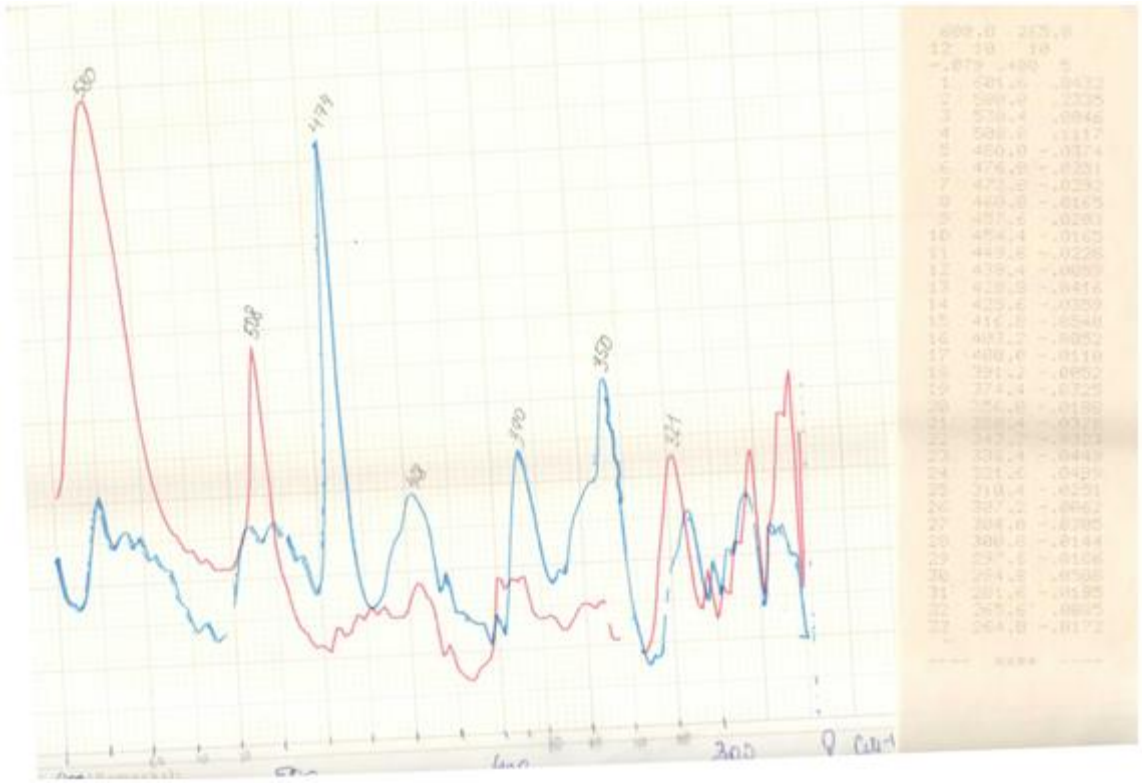

Fig. S17. IR **s**pectrum of complex **6b** in nujol: (blue line – **4c**, orange line – complex **6b**).

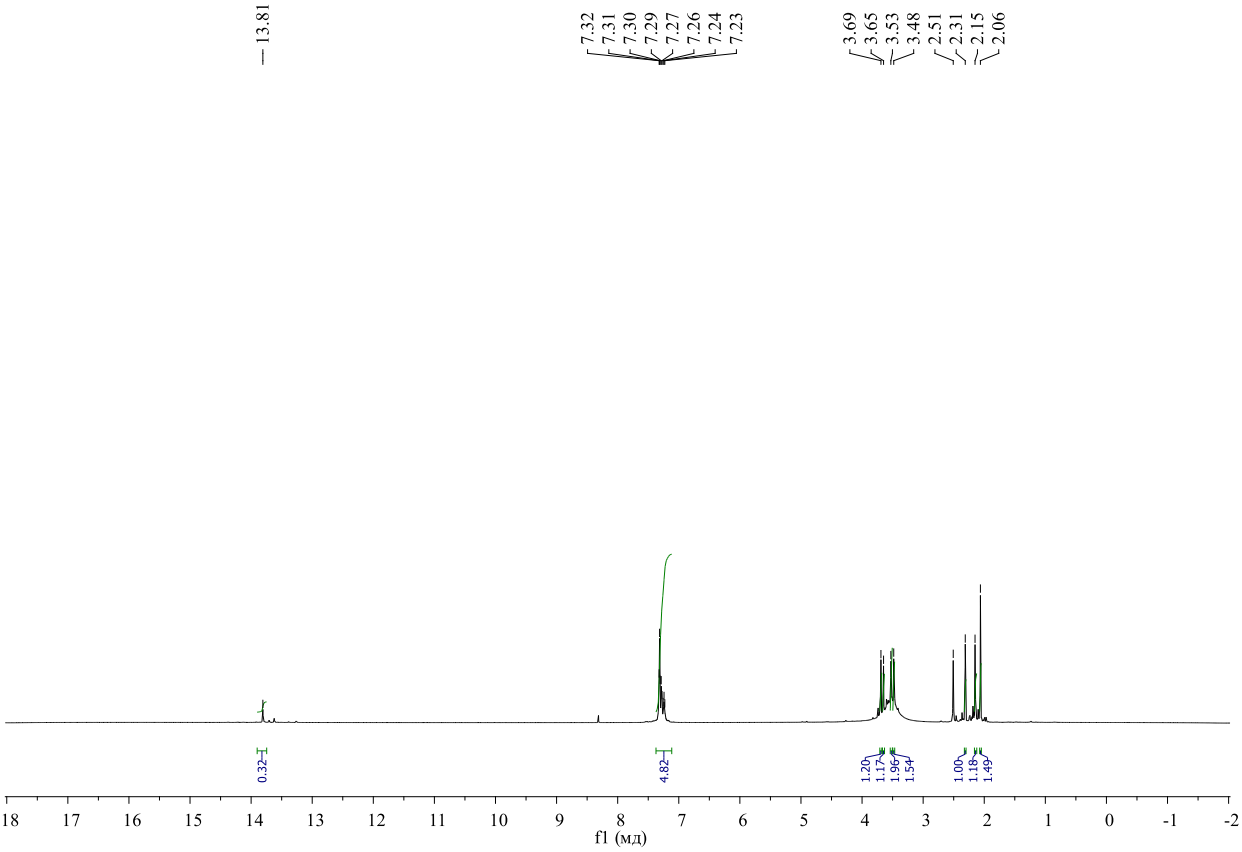

Fig. S18. ^{1}H NMR spectrum of complex **7** ($BnPzPtCl_2$) in DMSO-D_6 (500 MHz)

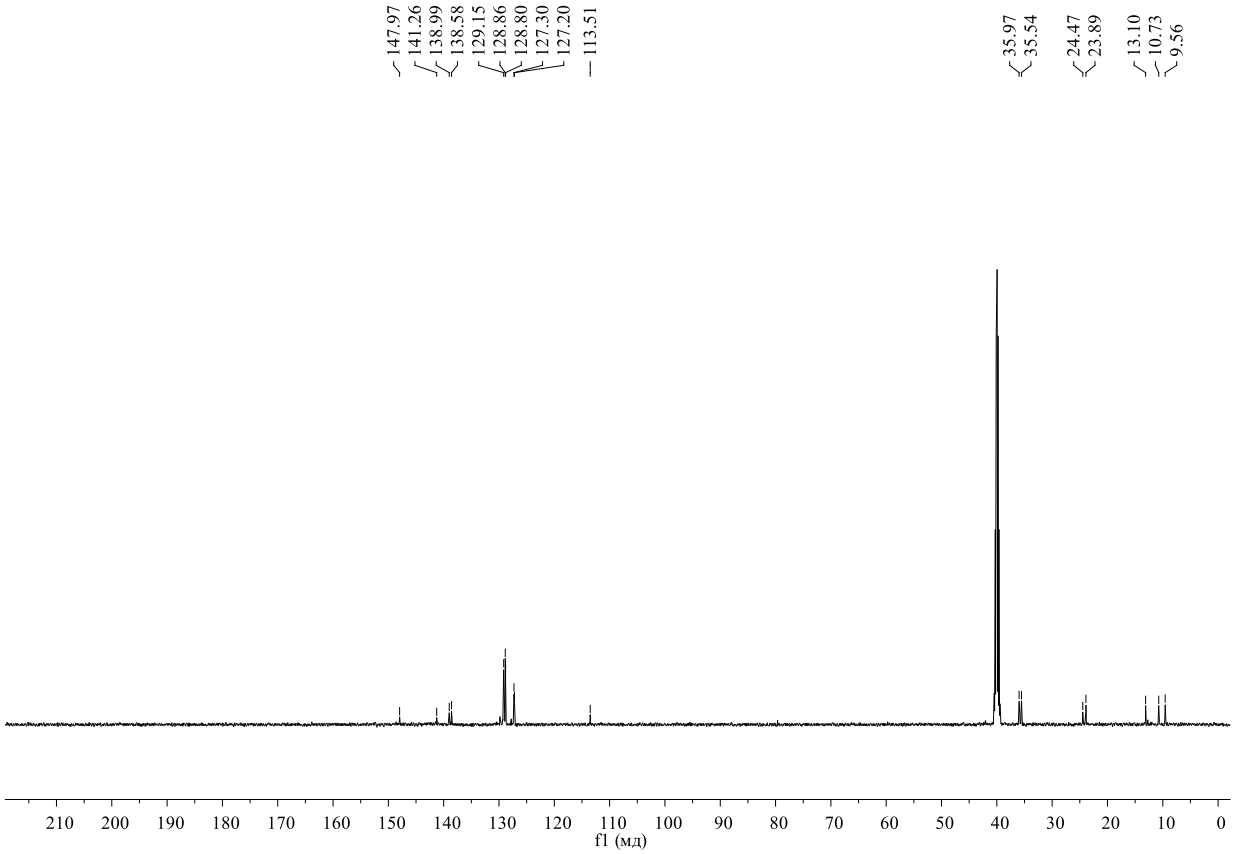

Fig. S19. ^{13}C NMR spectrum of complex **7** (BnPzPtCl$_2$) in DMSO-D$_6$ (125 MHz)

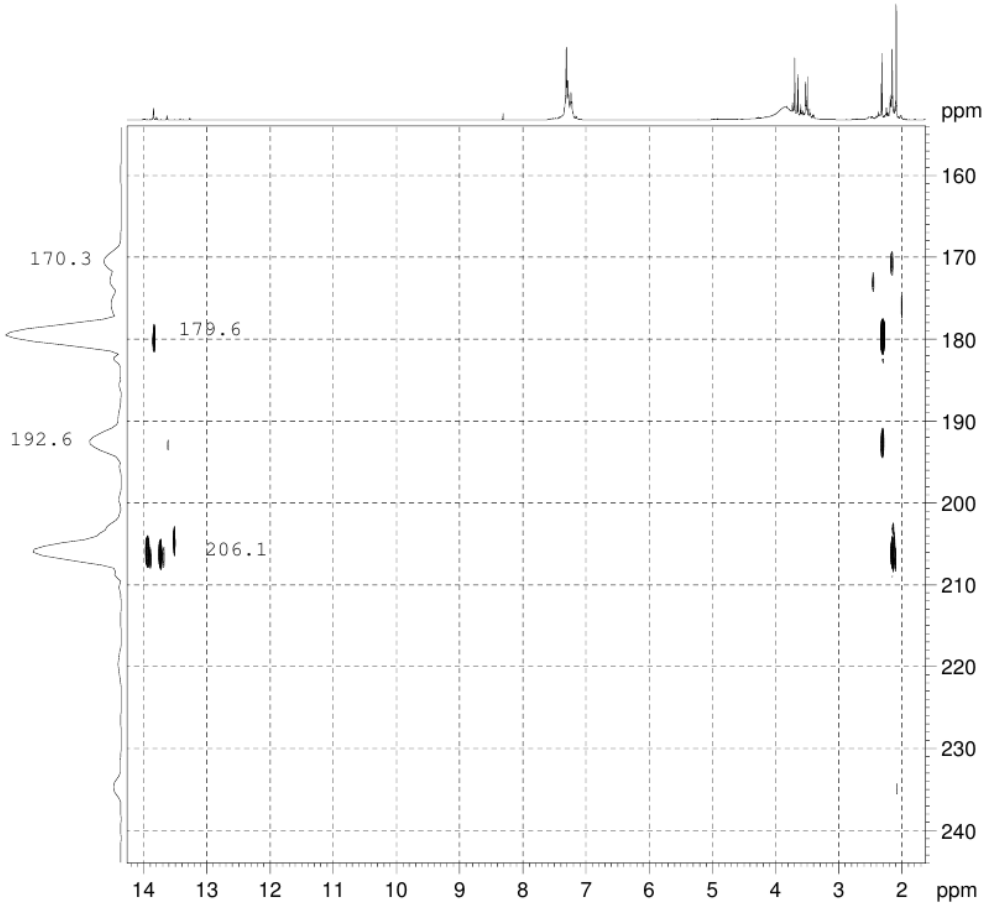

Fig. S20. ^{1}H-^{15}N-HMBC spectrum of complex **7** (BnPzPtCl$_2$) in DMSO-D$_6$ (500 MHz)

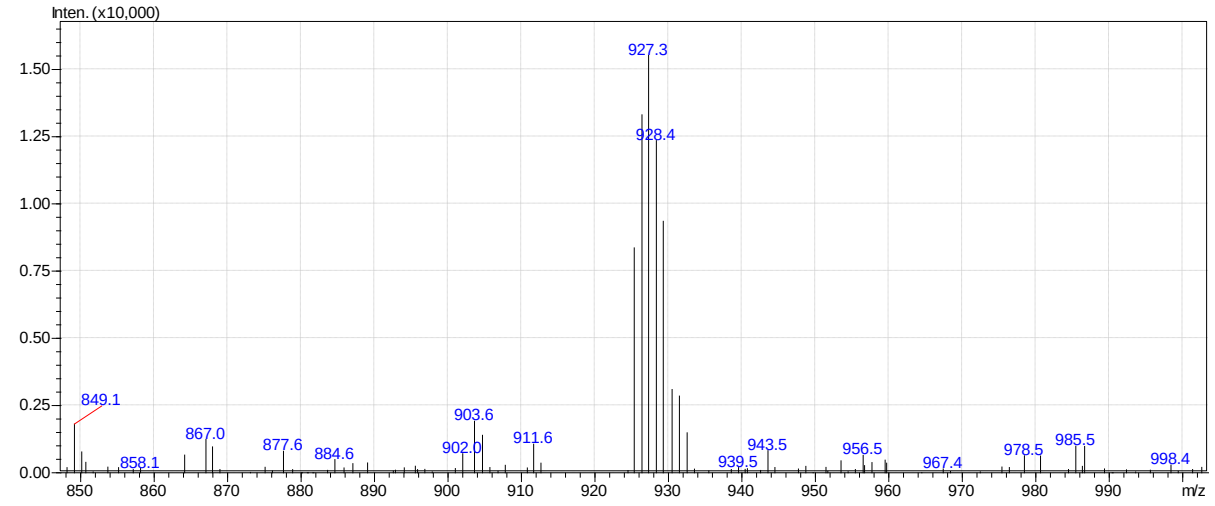

Fig. S21. Positive ion ESI mass spectrum of compound **7.**

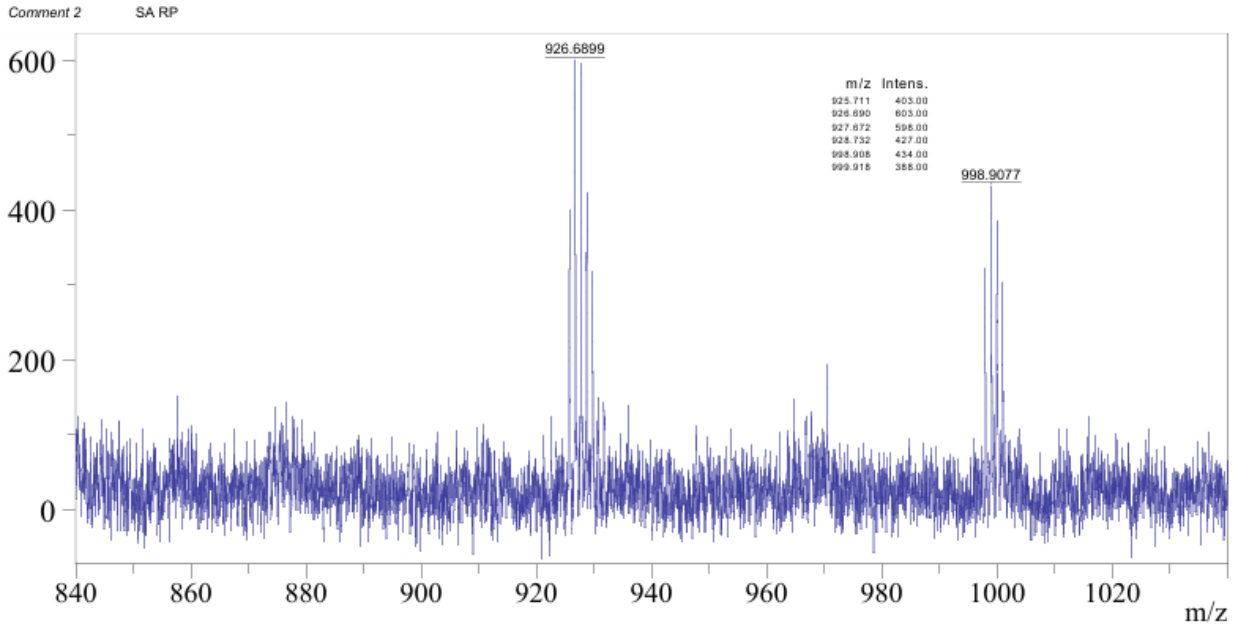

Fig. S22. Mass-spectrum MALDI TOF of compound **7** (sinapinic acid as a matrix).

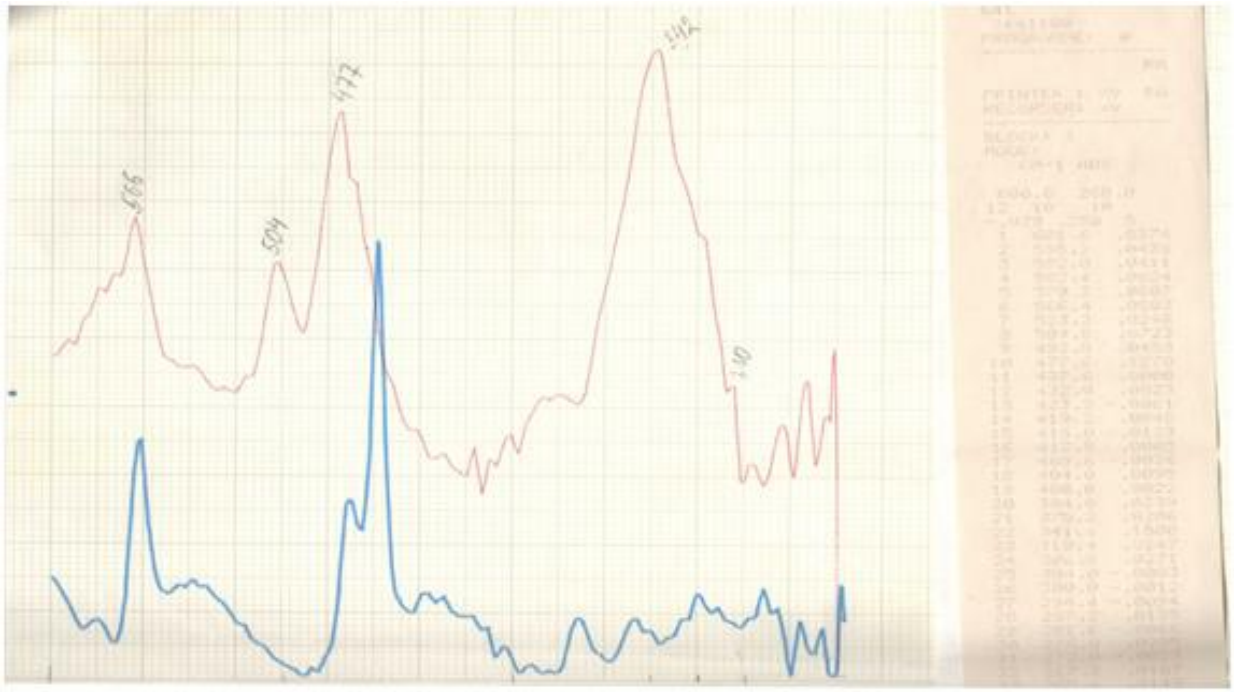

Fig. S23. IR spectrum of complex **7** in nujol: (blue line – **4b**, orange line – complex **7**).

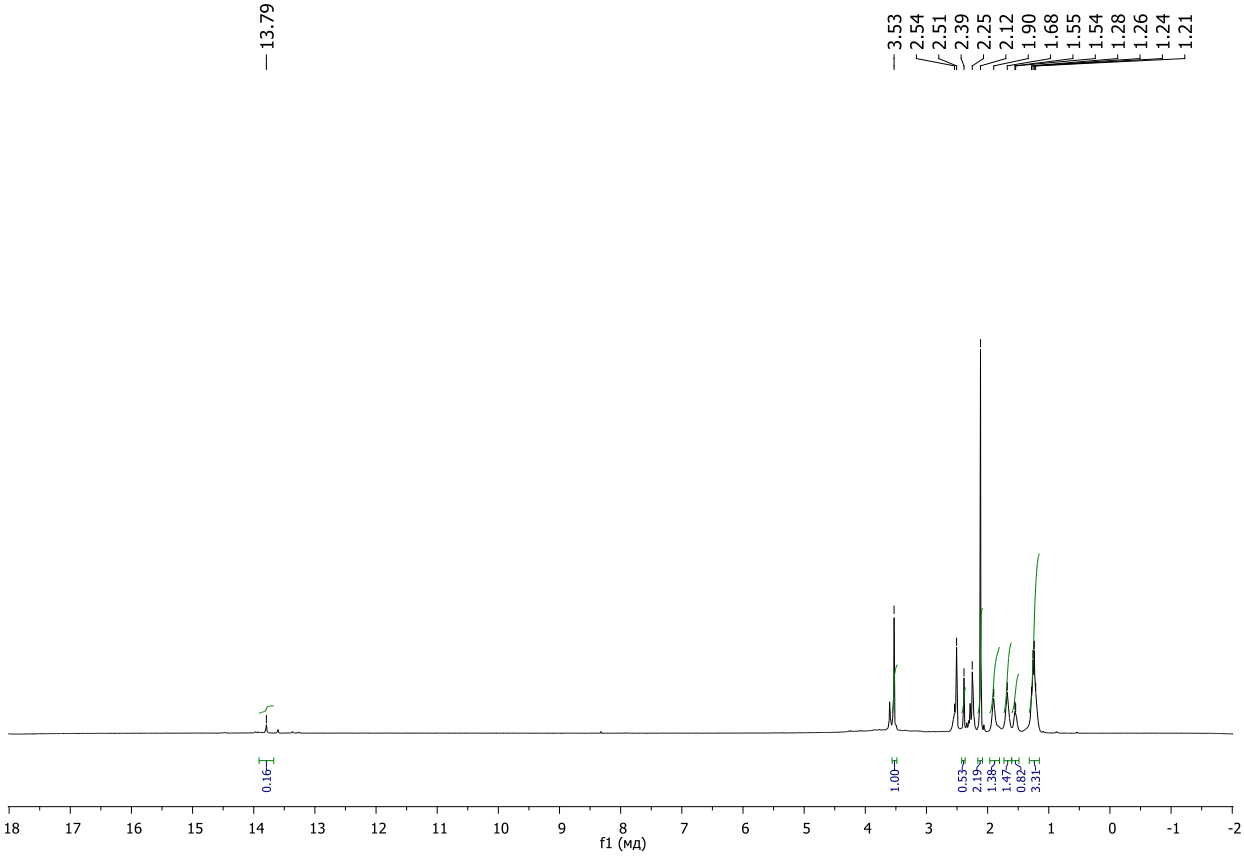

Fig. S24. ^{1}H NMR spectrum of complex **8 (**$CyPzPtCl_2$) in DMSO-D_6 (400 MHz)

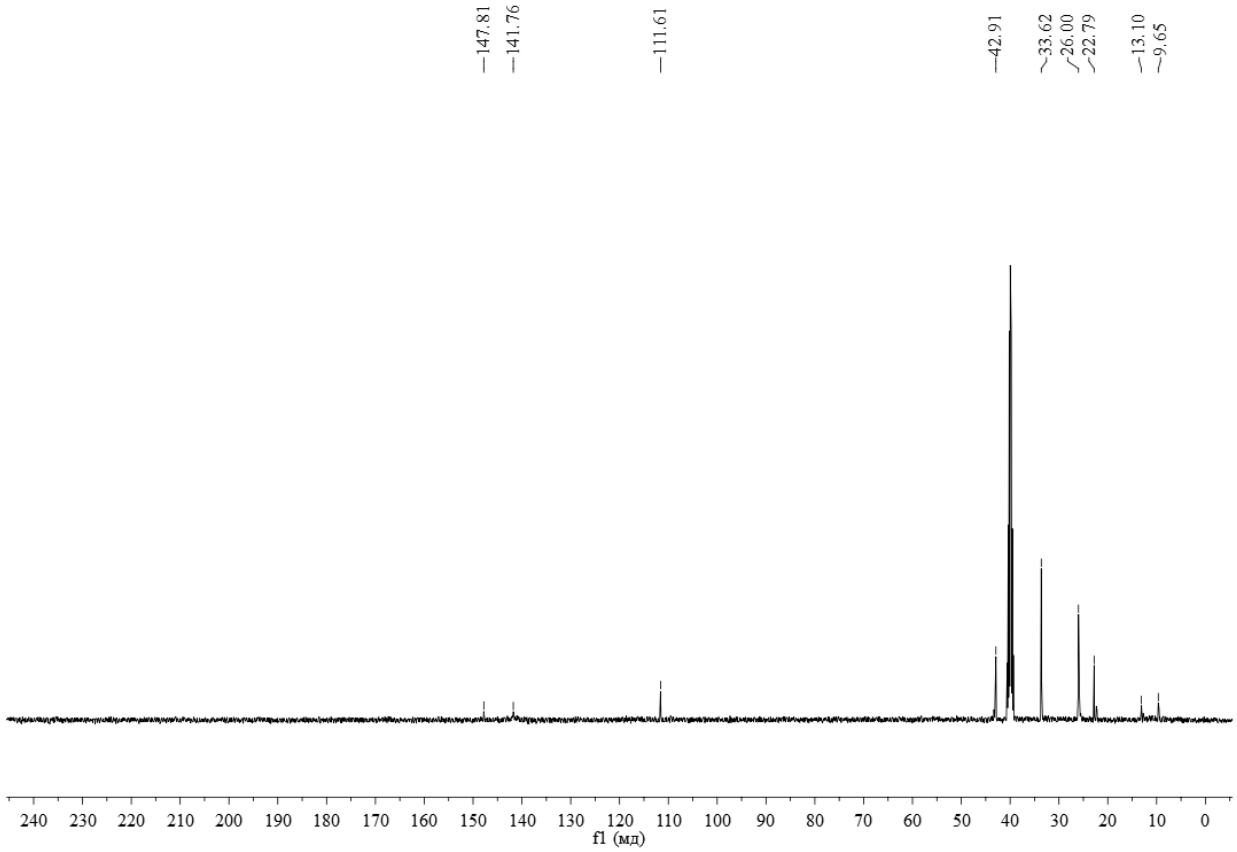

Fig. S25. ^{13}C NMR spectrum of complex **8 (**$CyPzPtCl_2$) in DMSO-D_6 (100 MHz)

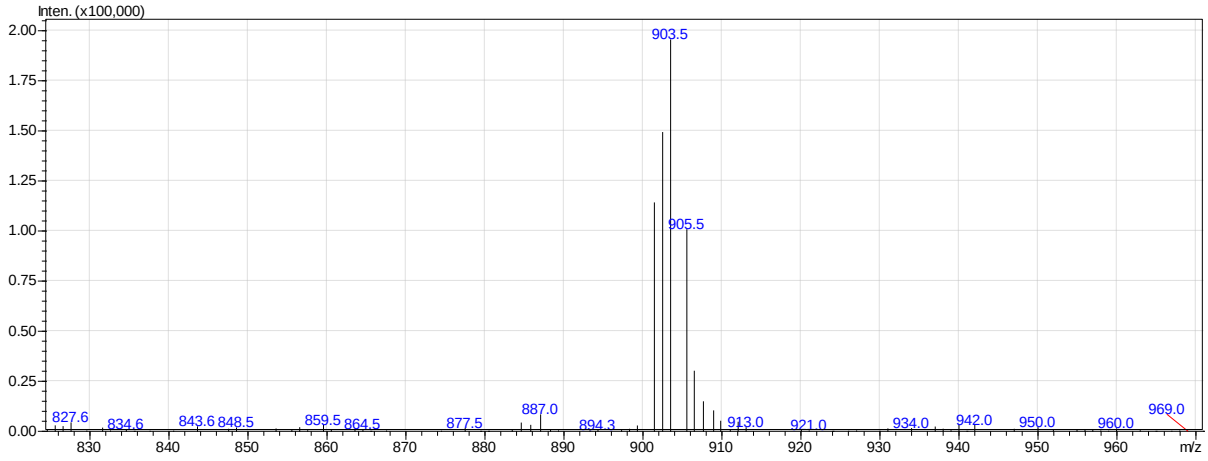

Fig. S26. Positive ion ESI mass spectrum of compound **8.**

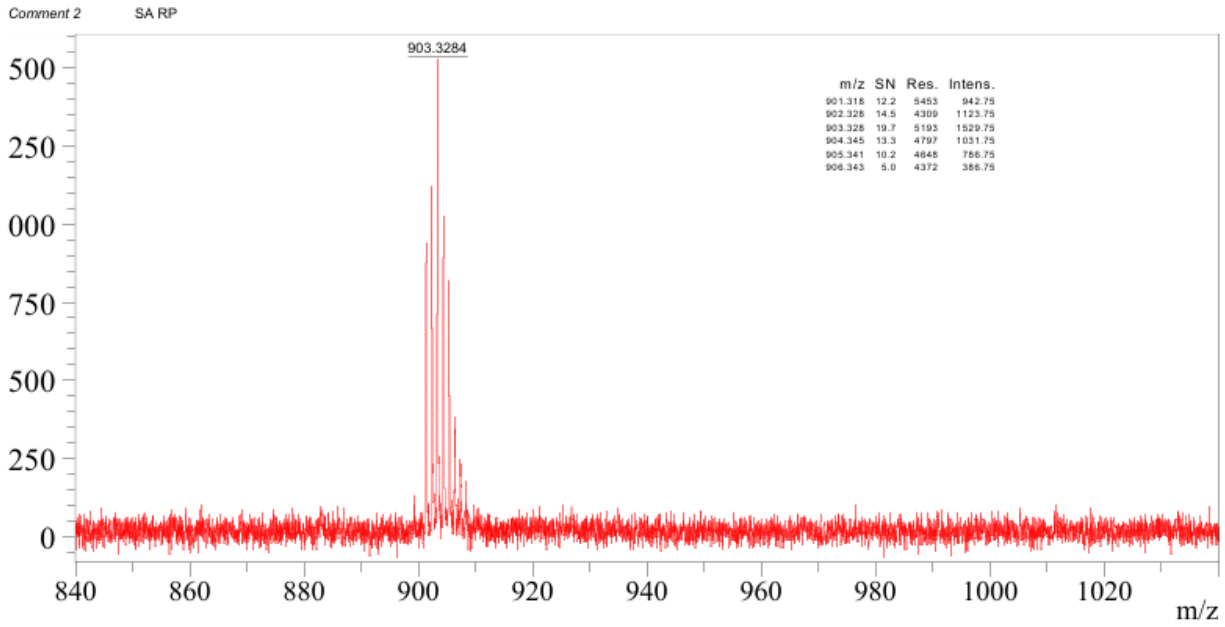

Fig. S27. Mass-spectrum MALDI TOF of compound **8** (sinapinic acid as a matrix).

Table S2 Partition coefficients (log P_{ow}) for compounds **4b** and **4c** experimentally determined by reversed phase HPLC.

Compounds	Log P_{ow}
4b	1.48 ± 0.4
4c	1.65± 0.3

Table S3 The **s**electivity index (SI) of neoplastic cells upon treatment with compounds **4a-d**, **5a**,**b**, **6a**,**b**, **7**,**8** and cisplatin

Compounds	**Jurkat**	**K562**	**U937**
4a	1.5	1.3	1.3
4b	2.4	1.5	1.4
4c	2.1	1.5	1.6
4d	1.8	1.4	1.5
5a	2.2	1.8	1.5
5b	1.7	1.4	1.4
6a	1.7	1.4	1.2
6b	4.5	3.7	3.1
7	6.7	1.6	1.6
8	12.5	2.8	2.5
cisplatin	1.4	1.8	1